iScience

CellPress
OPEN ACCESS

Article

# A time-space conversion method for material synthesis research

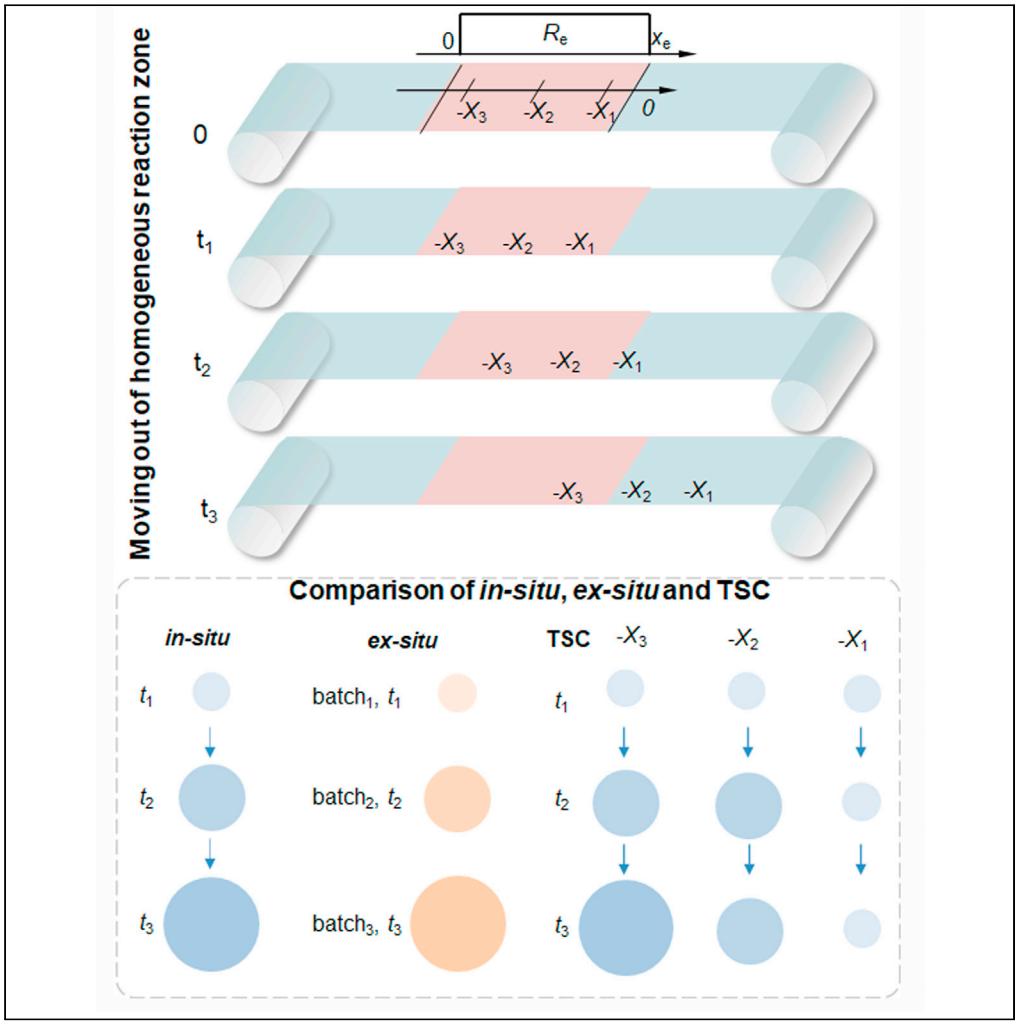


Yuting Hou, Minghao Liang, Fangzhu Qing, Xuesong Li

qingfz@uestc.edu.cn (F.Q.)
lxs@uestc.edu.cn (X.L.)

## Highlights

High-throughput time-space conversion method by adding a moving rate

Improving the efficiency and accuracy of research on material synthesis kinetics

Hou et al., iScience *24*, 103340
November 19, 2021 
https://doi.org/10.1016/j.isci.2021.103340

iScience

CellPress
OPEN ACCESS

Article

# A time-space conversion method for material synthesis research

Yuting Hou,[1,2] Minghao Liang,[1,2] Fangzhu Qing,[1,2,3,*] and Xuesong Li[1,2,3,4,*]

## SUMMARY

**Research on material synthesis is mostly performed through batch by batch testing with each corresponding to a set of parameters and a reaction time. Concurrent experiments that allow for multiple loadings throughout an inhomogeneous reaction zone provide a way to obtain high-throughput results. Here, a time-space conversion method is proposed. By sequentially passing a number of identical objects through a reaction zone, a significant diversity of reactions in one batch can be achieved depending on the spatial distribution and changes with time of the reaction zone. In particular, when the reaction zone is steady, the evolution of a reaction can be associated with the objects at their corresponding reaction stage. This greatly improves the efficiency and accuracy of research on material synthesis kinetics. This method may initiate a new wave of material synthesis research and accelerate the development of material science.**

## INTRODUCTION

Research on the synthesis of materials is mostly performed through batch by batch testing, where a single set of parameters are investigated per batch. Parallel experiments were addressed in the 19$^{th}$ century to discover suitable filament materials which greatly reduced cost and time (Hoogenboom et al., 2003; Maier, 2019). Because "a combinatorial approach" was put forward for high efficient material discovery, combinatorial and parallel techniques have been intensively developed (Xiang et al., 1995). Technologies such as high-throughput experiments (HTE) and high-throughput screening (HTS) have been used in various research fields, such as thin film material growth, high-entropy alloy design, biomaterials screening for stem cell differentiation, and rapid characterization technologies for electrochemical, thermal, optical, and catalytic properties (Chakraborty et al., 2017; Patel et al., 2016; Potyrailo et al., 2011; Wang et al., 2020). With the development of machine learning and artificial intelligence, high-throughput computation (HTC) is widely used in material design and synthesis (Curtarolo et al., 2013; Greeley et al., 2006; Jiang and Yang, 2021; Wilmer et al., 2011). HTC is an instructional method that utilizes machine learning and artificial algorithms for materials' data mining and database construction by supercomputers, which requires a large experimental database in order to increase predictive reliability and accuracy. The features of these high throughput methods are compared in Table 1.

Note that the reported high-throughput methods are mainly focused on the variety of materials and reaction conditions, whereas few on understanding the evolution of material synthesis, which is fundamental and crucial in understanding reaction kinetics and mechanisms. An *in-situ* study of reaction evolution is always preferred, but the reaction conditions and analytical comprehensiveness are limited by instrumentation (N'Diaye et al., 2009; Niu et al., 2013; Puretzky et al., 2013; Terasawa and Saiki, 2015; Wang et al., 2015). *Ex-situ* study is still the most common technique, and mainly consists of batch-by-batch testing, which is time-consuming and may be hindered by system fluctuations (Shen et al., 2018).

Here, a time-space conversion (TSC) method is proposed by sequentially passing a number of identical objects (e.g., substrates) through a reaction zone. By tuning the reaction conditions as a function of spatial distribution and time and the velocity of the substrates, a huge diversity of reactions in one batch can be achieved. In particular, when the reaction zone is steady (i.e., does not change with time), by tuning the way of the substrates passing through the reaction zone, the evolution of a reaction at each moment can be associated to the substrates with each corresponding to a reaction time or stage, which greatly improves the efficiency and accuracy of research on material synthesis kinetics. The TSC method may initiate a new wave of high throughput methods for material synthesis research and accelerate the development of material science.

[1]State Key Laboratory of Electronic Thin Films and Integrated Devices, University of Electronic Science and Technology of China, Chengdu 610054, China

[2]School of Electronic Science and Engineering, University of Electronic Science and Technology of China, Chengdu 610054, China

[3]Shenzhen Institute for Advanced Study, University of Electronic Science and Technology of China, Shenzhen 518110, China

[4]Lead contact

*Correspondence: qingfz@uestc.edu.cn (F.Q.), lxs@uestc.edu.cn (X.L.)

https://doi.org/10.1016/j.isci.2021.103340

**Table 1. Comparison of the high throughput methods**

| Method | Features | Refs. |
|---|---|---|
| HTE | Numeric parameters, multiple results | (Xiang et al., 1995) |
| HTS | Combinatorial characterizations, focused on parallel testing | (Chakraborty et al., 2017; Patel et al., 2016; Potyrailo et al., 2011; Wang et al., 2020) |
| HTC | Materials' data mining and database construction based on machine learning and artificial algorithm, reliability and accuracy depends on database | (Curtarolo et al., 2013; Greeley et al., 2006; Jiang and Yang, 2021; Wilmer et al., 2011) |
| TSC | An extension of HTE by moving the substrates, providing particular advantages for the study of reaction kinetics | This work |

## RESULTS AND DISCUSSION

### Theory

For simplicity, a one-dimensional system is considered where the reaction conditions are inhomogeneous in only one direction while homogeneous in the other two (e.g., by using a tubular reactor). Use $R$ to represent reaction conditions, which can be one or a combination of temperature, pressure, reactants, etc., $x$ to represent the spatial coordinate or the position in the system, and $t$ to represent the time with which the reaction goes on. Apparently, $R$ is a function of $x$ and $t$, represented as $R = r(x,t)$. As schematically shown in Figure 1A, a curved surface is used to show the general case in which $R$ is inhomogeneous and unsteady (i.e., it varies along with the position and changes with time). The reaction profile for a system (or a substrate) with a motion trace in the position-time plane corresponds to the projection of the reaction surface (the reaction trace) (Figure 1B). Likewise, the reaction profile as a function of time is the projection of the

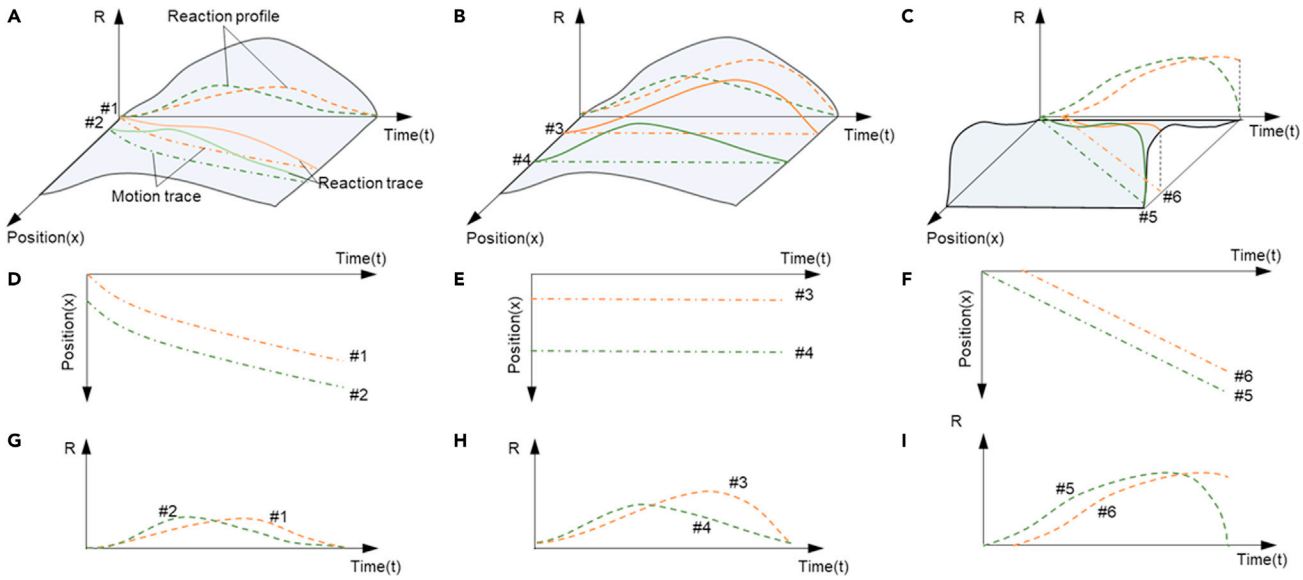


**Figure 1. Schematics of reaction conditions ($R$) as a function of spatial position ($x$) and reaction time ($t$)**

(A) General expression for inhomogeneous and unsteady reaction conditions. #1 and #2 represent two reactions starting from different positions and moving with the same velocity, respectively.

(B) Static reactions occur due to the substrate not moving, but due to inhomogeneous reactions conditions, #3 and #4 represent two reactions at different positions without moving, respectively.

(C) Steady reactions. By moving a number of substrates through the reaction zone at a constant velocity, the evolution of a reaction can be projected to the substrates, e.g., the green curve (#5) represents a full reaction while the orange curve (#6) represents an interrupted reaction by entering the reaction zone a little bit later.

(D, G, E, H, F, and I) Motion traces and reaction profiles corresponding to the reaction traces in A, B, and C, respectively. The solid, dash dot, and dash color lines represent reaction trace, motion trace, and reaction profile, respectively.

reaction trace in the reaction-time plane (Figure 1C). This can be expressed mathematically. Consider a substrate initially located at $x_0$ at time $t_0$ and moving at a velocity of $v$, which is not constant and a function of $t$, represented as $v = v(t)$. Then, the reaction profile as a function of $t$ is $R = r(x_0 + \int_{t_0}^{t} v(t)dt,\ t)$. It can be seen that different initial positions will cause different reaction profiles. For example, as shown in Figures 1A–1C, two substrates (or two positions on one substrate) labeled as #1 and #2 are initially located at two different positions, $x_1$ and $x_2$, respectively. They start to move simultaneously at $t_0$ at the same velocity. The reaction profiles of #1 and #2 are $r(x_1 + \int_{t_0}^{t} v(t)dt,\ t)$ and $r(x_2 + \int_{t_0}^{t} v(t)dt,\ t)$, respectively. By simultaneously moving a number of substrates from different initial positions in an inhomogeneous and unsteady reaction zone, a diversity of reaction profiles, normally resulting in different final product, can be achieved, which is essentially a high throughput method as well.

Compared to the traditional static HTE method which carries out spatially distributed parallel experiments to achieve multiple reaction profiles, the TSC method is extended to experiments in the time space. This provides great advantages for studies on reaction kinetics, as will be further discussed below.

## Examples

Some specific cases and application examples of the TSC methods are discussed below, explicated with the chemical vapor deposition (CVD) of graphene films on Cu foils (Li et al., 2009a).

(1) **Substrates are static and the conventional HTE.** This is actually the normal reaction process where the substrates are static and the spatially inhomogeneous reaction changes with time (Figures 1D–1F). The reaction trace is parallel to the $R$-$t$ plane, i.e., $v = 0$. If a number of substrates are statically located at different positions corresponding to different reaction conditions, then this is the common HTE method, i.e., spatially distributed parallel experiments, $R_i = r(x_i,\ t)$, where $x_i$ is independent of $t$.

(2) **Steady reaction conditions.** The reaction conditions do not change with time and thus the reaction plot can be simplified as $R = r(x)$, as shown in Figures 1F, 1G, and 2A. Reaction zone is restricted within the spatial interval $[0, x_e]$. Mathematically, $R = 0$ for $x<0$ or $x>x_e$ and $R = r(x)$ for $0 \le x \le x_e$. If a substrate passes through the reaction zone from left to right at a constant velocity of $v$, then the reaction profile for the substrate versus $t$ is $R = r(vt)$. This is analogous to a normal static reaction process, as shown in Figure 2B. The reaction evolution stage at time $t_j$ in Figure 2B corresponds to the same reaction stage at position $x_j$ in Figure 2A with a relationship of $t_j = x_j/v$.
Now consider a strip of substrate, as shown in Figure 2C. The left end of the substrate is represented with $X_0$ and the right end with $X_n$. A position on the substrate is represented with $X_i$. Initially, $X_0$ is located at $-x_e$, $X_n$ at 0, and $X_i$ at $x_i$ (note $x_i$ is negative). Let the substrate move toward the reaction zone. Once the whole substrate enters the reaction zone (consequently, now $X_0$ at 0, $X_n$ at $x_e$, and $X_i$ at $x_e + x_i$), the reaction is terminated. Then the reaction result of a position on the substrate, $X_i$, corresponds to the moment $t_i = (x_e + x_i)/v$ during the evolution of the reaction process (Figure 2E). Therefore, the reaction evolutions corresponding to different times or stages are projected to the spatially distributed positions on a substrate, i.e., the conversion between time and space for kinetics research is established, with which the investigation on reactions as a function of time can be performed with only one batch. This is also why this method is referred to as TSC. Note that isolated substrates located in line and move at the same velocity work in the same way.
The time to space conversion can be conducted in another way. Let the substrate initially be located within the reaction zone and then start the reaction. Have the substrates move so that they will ultimately leave the reaction zone (Figure 2D). The reaction profile for a position on the substrate, $X_i$, which is initially located at $x_i$, is shown in Figure 2F. This can be used to study graphene growth kinetics, which is usually performed in the time-consuming batch-by-batch method (Kim et al., 2012; Li et al., 2010).
A typical graphene synthesis process is schematically shown in Figure 3A. The Cu substrate is heated up to a desired temperature in an Ar or Ar/$H_2$ mixture atmosphere and annealed for a specific time. Methane is then introduced to trigger the graphene growth reaction. If the gas atmosphere is unchanged during the cooling down process (Li et al., 2009a), the reaction profile can be seen as $T$ v.s. $t$

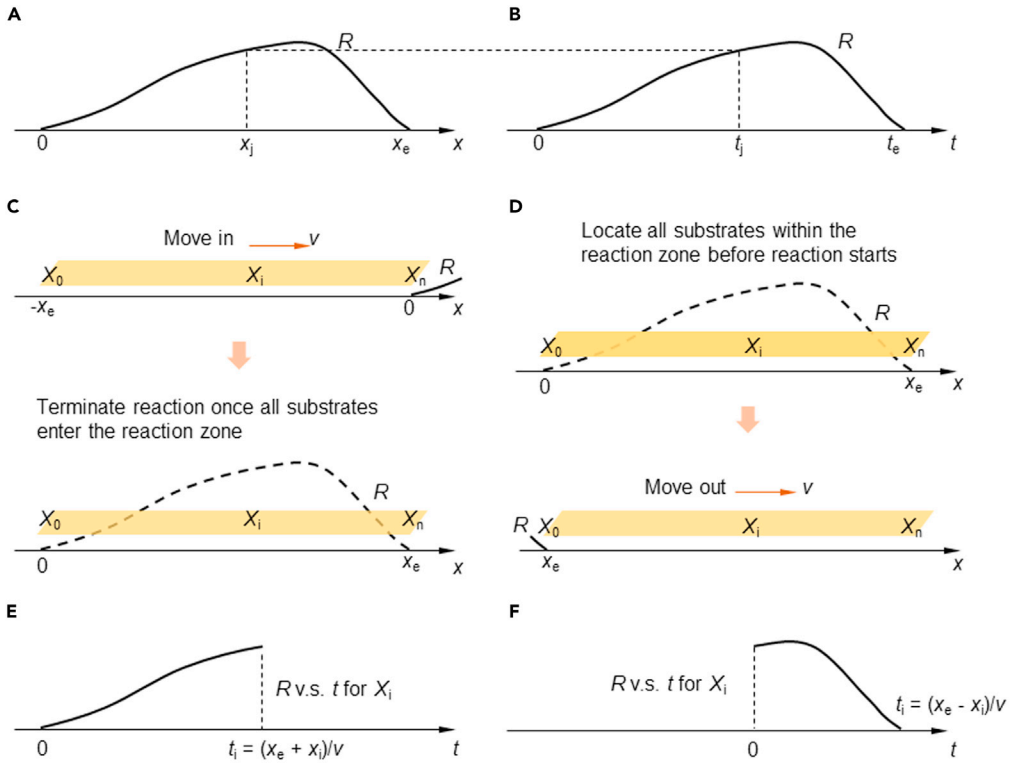


**Figure 2. Steady reaction**

(A) Spatially distributed steady reaction profile.

(B) Unsteady reaction profile for a static site.

(C) Conversion of reaction stages to spatial positions by moving systems into the reaction zone. The dash reaction profile represents the reaction that has been terminated.

(D) Conversion of reaction stages to spatial positions by moving systems out of the reaction zone. The dash reaction profile represents the reaction that has begun.

(E) Reaction profile for the case of (C).

(F) Reaction profile for the case of (D).

starting from the time when the methane is on and ending when the temperature is low enough for the reaction rate to be negligible. If methane is shut off during the cooling down process (Kim et al., 2012), the reaction profile needs to include the change in gas atmosphere. Because it is difficult to determine the lower limit of temperature, neither can give a clear endpoint of the reaction. In practice, the reaction during the cooling down process is normally neglected if the cooling down process is rapid.

The TSC method takes the cooling down process into account. As schematically shown in Figure 3B, a Cu strip was loaded in the center zone of a tubular furnace. The origin of the coordinate is set at the right end of the furnace. The Cu substrate was initially heated up and annealed, similar to the standard process. Then it started to move just after introducing 50 sccm $CH_4$/Ar (1% $CH_4$ diluted in Ar). The motion could be realized by either using a roll-to-roll system to move the substrate or a sliding rail furnace to move the furnace. Figure 3C shows the reaction profiles of some positions and Figure 3D shows the optical microscopy images of the corresponding as-grown graphene on Cu.

Figure 3E shows that the nucleation density at section > −27 cm is quite high and significantly lower at the < −33 cm position. From Figure 3C it can be seen that the reaction temperature of section > −27 cm is low and that of section < −33 cm is high. Thus, it can be concluded that high temperature is preferred to suppress the nucleation density and that the nucleation kinetics at high and low temperatures are different. In addition, if the temperature in the center zone is approximately uniform for positions < −33 cm, the difference between the reaction results with time (the distance between positions divided by the moving velocity of the substrate) can be analogous to the reaction rate. From Figure 3E it can be seen that the nucleation rate is almost zero, whereas the increase of coverage as shown in Figure 3F indicates that graphene keeps growing. This can be attributed to the higher

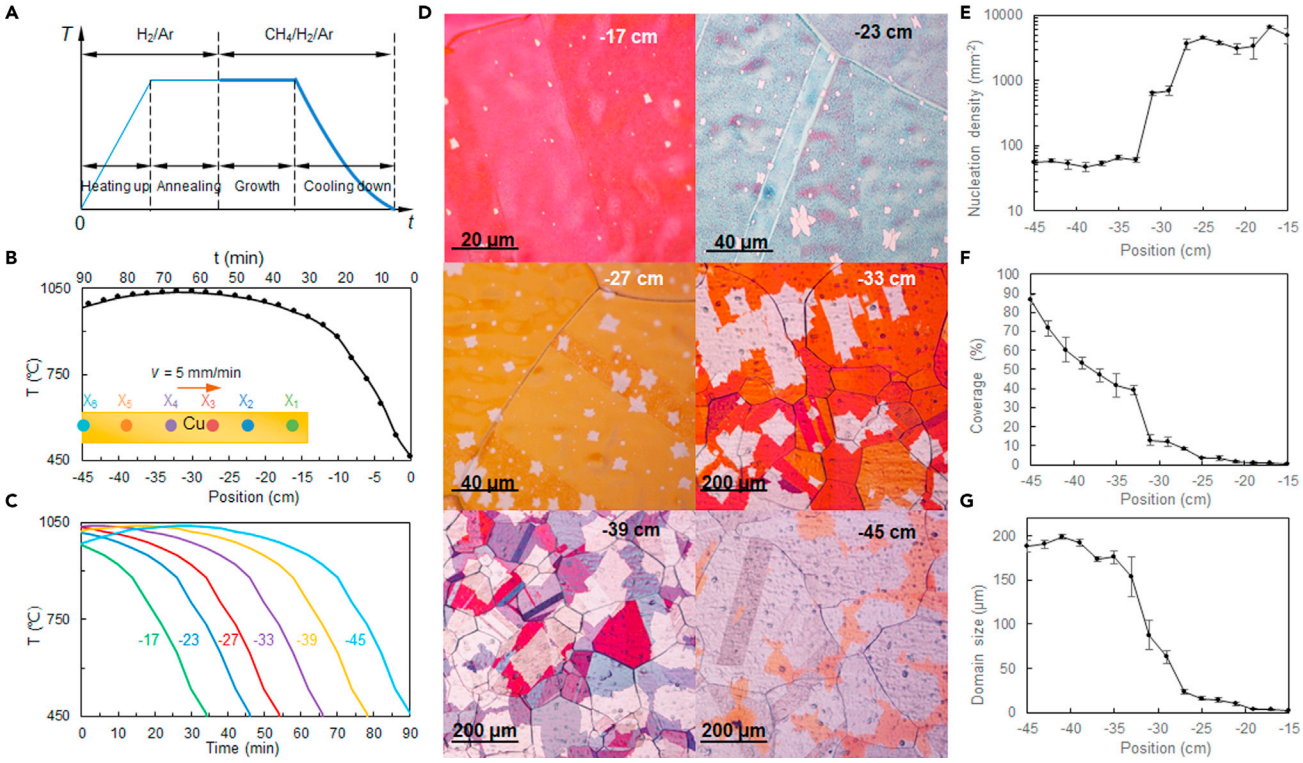


**Figure 3. Investigation of growth kinetics with TSC**

(A) Schematics of the experimental process for normal graphene synthesis. The bold blue plot is the reaction profile represented with *T*.

(B) Temperature distribution representing the reaction zone. The origin of the position is set at the right end of the zone. The orange rectangular bar schematically shows the initial location of the Cu substrate. The top axis is the time for the corresponding position to move out of the furnace zone at 5 mm/min.

(C) Reaction profiles of the labeled sites shown in (B) with corresponding color, and (D), corresponding optical microscopy images of as-grown graphene on Cu after slightly baking in air.

(E–G) Plots of nucleation density, coverage, and domain size v.s. position, respectively.

energy barrier (or equilibrium concentration of active species) of nucleation than that of growth. With the decrease of partial pressure of methane, i.e., the supply rate of C precursor, the reaction can be: I. Nucleation density increases with time, II. Nucleation density does not change and domains can keep growing into a completed film, or III. Nucleation density does not change and there is a limit of growth before completed growth (Li et al., 2010, 2012). Although completed growth when moving the substrate has not been achieved because of the limitation of the length of the heating zone, completed growth has been demonstrated in a normal static process with the same gas parameters (results not shown), indicating the current methane flow is in reaction scenario II. Figure 3G shows graphene domain growth with time. However, with more and more domains merging together, the determination of domain size becomes less accurate.

Graphene growth kinetics have been studied for a long time and the above conclusions are not novel. However, it should be noted that all these deductions are only from the results produced in one batch. The advantage of the TSC method is evident for a high-throughput data collection.

(3) **Unsteady reaction.** When the reaction conditions change with time, i.e., an unsteady reaction, moving the substrates provides a more diverse representation of reactions. Figure 4A shows the reaction profiles of some sites on a Cu strip moving in the same way as that in Figure 3B with an unsteady reaction. The difference is that in Figure 3B the atmosphere does not change with time and thus its dependency is not necessary to show in those reaction profiles, whereas in Figure 4A methane flow increases step by step from 40 to 50 and then to 60 sccm with each flow rate lasting for 50 min, 20 min, and 20 min, respectively. Therefore, the reaction profiles are the superposition of temperature and methane flow rate. Figure 4B shows the optical microscopy characterization results of the corresponding as-grown graphene on Cu. Figures 4C–4E show graphene nucleation density,

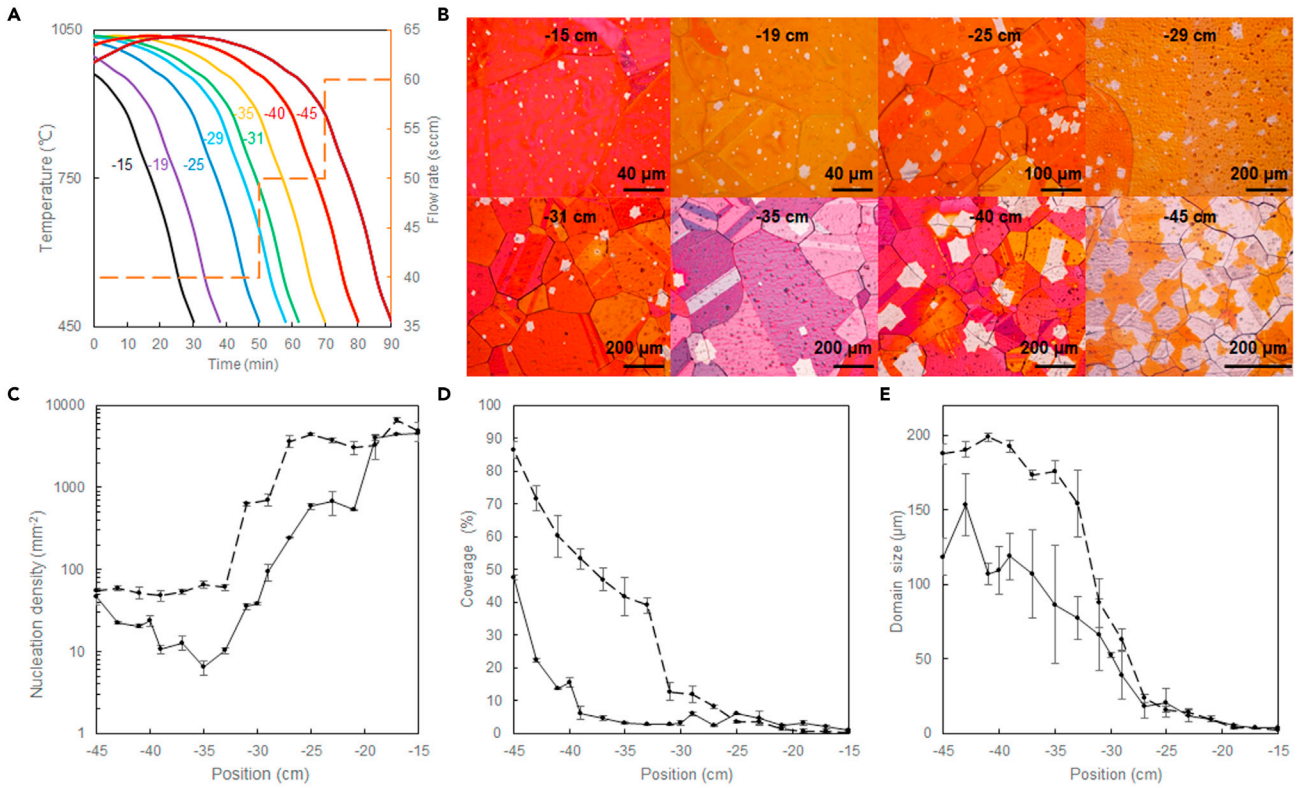


**Figure 4. Investigation of multiple-step growth with TSC**

(A) Reaction profiles of some positions and (B), corresponding optical microscopy images of as-grown graphene on Cu after slightly baking in air. (C–E) Plots of nucleation density, coverage, and domain size v.s. position, respectively. The dash curves are the results of the steady reaction, duplicated here for comparison.

coverage, and domain size, respectively, as a function of position on the Cu strip. Those of the steady reaction are also shown with a dash plot for comparison. It can be seen that initially both the nucleation density and growth rate are lower than those of the steady reaction with 50 sccm $CH_4$/Ar, which can be attributed to the smaller $CH_4$/Ar flow (40 sccm). Then the nucleation density increases with the increase of $CH_4$/Ar flow. The larger deviation of domain sizes in Figure 4E also indicates the new nucleation because of the equilibrium break with the increase of $CH_4$/Ar flow. At the end, a larger $CH_4$/Ar flow (60 sccm) results in a higher growth rate, as indicated by the steeper increase of the coverage shown in Figure 4D.

## Error analysis and extension

In present work we used graphene synthesis, particularly, monolayer graphene synthesis, as an example to demonstrate the application of the TSC method. This is because the growth kinetics of monolayer graphene has been well investigated. However, the TSC idea can be applied to a much broader field. The key issue is the determination of reaction conditions or the modification of reaction apparatus.

In the above examples of graphene growth, the reaction conditions are assumed spatially homogeneously distributed except temperature. However, in practice there are always some gas phase reactions, resulting in the increase of the active species from methane decomposition along with gas flow direction (Li et al., 2012). Because methane is mainly decomposed catalytically on the surface of Cu, when the partial pressure of methane is low, the pyrolysis can be neglected. If the partial pressure of methane is high, the pyrolysis has to be considered. This issue can be resolved by specifically designing the way that gas is fed into the system.

Another issue is the determination of the reaction boundary because of the temperature gradient from the hot reaction zone to room temperature zone. In the case of graphene as shown in Figure 3, the graphene

growth reaction started at a high temperature and then experienced a continuous decrease of temperature. The reaction rate decreased rapidly and approached zero with the decrease of temperature. It is difficult to determine exactly the temperature where the reaction stops. However, because the rate is exponentially related to temperature, normally a "reasonable" small reaction rate can be taken as zero (the boundary of the reaction zone). Whether it is "reasonable" depends on whether it results in big errors. For example, in Figure 3, the coverage of graphene at −17 cm is very close to zero. Taking this position as the boundary of the reaction zone does not affect the main conclusions. In fact, the effect of reaction boundary can be suppressed by increasing the velocity of the substrate.

By tuning the gas parameters, the growth of multilayer graphene can be investigated. It has been well acknowledged that graphene growth on Cu is self-limited (Li et al., 2009b). That is, once the Cu surface is fully covered by graphene, the reaction stops. The traditional batch-by-batch process is difficult to identify if the graphene adlayers are grown before or after the complete growth of the first graphene layer. It may be conducted by growing monolayer graphene first in one batch and then growing adlayers with a longer reaction time in another batch. This is indirect and time consuming. The fluctuation from batch to batch also complicates the results. With the TSC method, the evolution of graphene adlayers can be tracked easily in one batch.

Synthesis of h-BN or $MoS_2$ 2D films by CVD is similar to graphene but using solid the precursors, which are normally heated in a separated heating zone away from the reaction zone and then transport in gas phase (Lee et al., 2012; Wu et al., 2013). For this case, the effect of pressure is more significant. The lower the pressure, the larger the mean free path of the gas molecules, and therefore the more uniform gas distribution. For the MBE process, the apparatus may need to be specially designed so that a batch of substrates can be loaded for reaction and then removed out of the reaction zone one by one while without interrupting the reaction.

The TSC method is also suitable to study bulk materials. For example, by pulling a long metal rod out of the high temperature zone and quenching it when one end of the rod is cooled down to almost room temperature while the other end is still at the high temperature, the phase transition of metal from high to low temperatures is therefore frozen along with the rod.

The TSC method shows great advantages for reactions with extreme conditions such as high temperature and/or high vacuum, where normally solid substrates are used. It takes time to build up the reaction conditions while the TSC method can investigate the reaction evolution in one batch instead of using multiple experiments. Gas or liquid reactions usually occur in mild conditions and the reaction can be easily tracked. However, the TSC method is not restricted to specific substrates or reaction systems, as long as the reaction conditions are clearly determined and the apparatus is appropriately designed.

## Conclusions

This report showcased an additional approach to high throughput methods. By moving the substrates through the reaction zone, a more diverse reaction profile can be achieved when compared to the traditional static combinatorial approach. In addition, the velocity bridges time and space (i.e., the distance between two substrates). Therefore, the results of two moving substrates (or at two different initial positions on one substrate) can be analogous to the results for two corresponding moments in the static reaction. This makes it more efficient to study reaction kinetics by projecting the evolution of a reaction to spatially distributed positions in one batch as opposed to batch-by-batch testing. Another advantage of the one-batch TSC method is that it is not affected by system fluctuation, which affects the reproducibility from batch to batch. The reliability of the TSC method depends on the control of the reaction conditions, which can be achieved by an appropriate design of the system. Therefore, the TSC method may pave a new way for materials synthesis research and significantly accelerate the progress of materials science.

## Limitation of the study

The key to utilizing the TSC method is the determination of reaction conditions or the modification of reaction apparatus. However, in practice, it is difficult to completely control or determine the reaction zone. The reaction conditions are approximated. The difference between the actual distribution of reaction conditions and the ideal situation must be considered.

## STAR★METHODS

Detailed methods are provided in the online version of this paper and include the following:

- KEY RESOURCES TABLE
- RESOURCE AVAILABILITY
  - Lead contact
  - Materials availability
  - Date and code availability
- METHODS DETAILS
  - Equipment and graphene growth
  - Optical microscopy
- QUANTIFICATION AND STATISTICS ANALYSIS
  - Image analysis and domain number counting

## ACKNOWLEDGMENTS

This work was supported by the National Natural Science Foundation of China (No. 51772043 and 51802036) and Shenzhen Science and Technology Program (No. (2021)105). The authors acknowledge Dr. Richard C. Stehle for his editing the manuscript and fruitful comments.

## AUTHOR CONTRIBUTIONS

X.L. and F.Q. conceived the project. X.L. and Y.H. designed the study. Y.H. and M.L. performed the experiments, data acquisition. X.L. and Y.H. wrote the manuscript. All authors discussed and commented on the manuscript.

## DECLARATION OF INTERESTS

The authors declare that they have no conflict of interest.

Received: August 25, 2021
Revised: October 5, 2021
Accepted: October 21, 2021
Published: November 19, 2021

## REFERENCES

Chakraborty, S., Xie, W., Mathews, N., Sherburne, M., Ahuja, R., Asta, M., and Mhaisalkar, S.G. (2017). Rational design: A high-throughput computational screening and experimental validation methodology for lead-free and emergent hybrid perovskites. ACS Energy Lett. *2*, 837–845. https://doi.org/10.1021/acsenergylett.7b00035.

Curtarolo, S., Hart, G.L., Nardelli, M.B., Mingo, N., Sanvito, S., and Levy, O. (2013). The high-throughput highway to computational materials design. Nat. Mater. *12*, 191–201. https://doi.org/10.1038/nmat3568.

Greeley, J., Jaramillo, T.F., Bonde, J., Chorkendorff, I.B., and Norskov, J.K. (2006). Computational high-throughput screening of electrocatalytic materials for hydrogen evolution. Nat. Mater. *5*, 909–913. https://doi.org/10.1038/nmat1752.

Hoogenboom, R., Meier, M.A.R., and Schubert, U.S. (2003). Combinatorial methods, automated synthesis and high-throughput screening in polymer research: Past and present. Macromol. Rapid Commun. *24*, 16–32. https://doi.org/10.1002/marc.200300147.

Jiang, S., and Yang, K. (2021). Review of high-throughput computational design of Heusler alloys. J. Alloys Compd. *867*. https://doi.org/10.1016/j.jallcom.2021.158854.

Kim, H., Mattevi, C., Calvo, M.R., Oberg, J.C., Artiglia, L., Agnoli, S., Hirjibehedin, C.F., Chhowalla, M., and Saiz, E. (2012). Activation energy paths for graphene nucleation and growth on Cu. ACS Nano *6*, 3614–3623. https://doi.org/10.1021/nn3008965.

Lee, K.H., Shin, H.J., Lee, J., Lee, I.Y., Kim, G.H., Choi, J.Y., and Kim, S.W. (2012). Large-scale synthesis of high-quality hexagonal boron nitride nanosheets for large-area graphene electronics. Nano Lett. *12*, 714–718. https://doi.org/10.1021/nl203635v.

Li, X., Cai, W., An, J., Kim, S., Nah, J., Yang, D., Piner, R., Velamakanni, A., Jung, I., Tutuc, E., et al. (2009a). Large-area synthesis of high-quality and uniform graphene films on copper foils. Science *324*, 1312–1314. https://doi.org/10.1126/science.1171245.

Li, X., Cai, W., Colombo, L., and Ruoff, R.S. (2009b). Evolution of graphene growth on ni and cu by carbon isotope labeling. Nano Lett. *9*, 4268–4272. https://doi.org/10.1021/nl902515k.

Li, X., Magnuson, C.W., Venugopal, A., An, J., Suk, J.W., Han, B., Borysiak, M., Cai, W., Velamakanni, A., Zhu, Y., et al. (2010). Graphene films with large domain size by a two-step chemical vapor deposition process. Nano Lett. *10*, 4328–4334. https://doi.org/10.1021/nl101629g.

Li, Z., Zhang, W., Fan, X., Wu, P., Zeng, C., Li, Z., Zhai, X., Yang, J., and Hou, J. (2012). Graphene thickness control via gas-phase dynamics in chemical vapor deposition. J. Phys. Chem. C *116*, 10557–10562. https://doi.org/10.1021/jp210814j.

Maier, W.F. (2019). Early years of high-throughput experimentation and combinatorial approaches in catalysis and materials science. ACS Comb. Sci. *21*, 437–444. https://doi.org/10.1021/acscombsci.8b00189.

N'Diaye, A.T., van Gastel, R., Martinez-Galera, A.J., Coraux, J., Hattab, H., Wall, D., zu Heringdorf, F.-J.M., Horn-von Hoegen, M., Gomez-Rodriguez, J.M., Poelsema, B., et al. (2009). In situ observation of stress relaxation in epitaxial graphene. New J. Phys. *11*, 113056. https://doi.org/10.1088/1367-2630/11/11/113056.

Niu, T., Zhou, M., Zhang, J., Feng, Y., and Chen, W. (2013). Growth intermediates for CVD graphene on Cu(111): Carbon clusters and defective graphene. J. Am. Chem. Soc. *135*, 8409–8414. https://doi.org/10.1021/ja403583s.

Patel, A.K., Tibbitt, M.W., Celiz, A.D., Davies, M.C., Langer, R., Denning, C., Alexander, M.R., and Anderson, D.G. (2016). High throughput screening for discovery of materials that control stem cell fate. Curr. Opin. Solid State Mater. Sci. *20*, 202–211. https://doi.org/10.1016/j.cossms.2016.02.002.

Potyrailo, R., Rajan, K., Stoewe, K., Takeuchi, I., Chisholm, B., and Lam, H. (2011). Combinatorial and high-throughput screening of materials libraries: review of state of the art. ACS Comb. Sci. *13*, 579–633. https://doi.org/10.1021/co200007w.

Puretzky, A.A., Geohegan, D.B., Pannala, S., Rouleau, C.M., Regmi, M., Thonnard, N., and Eres, G. (2013). Real-time optical diagnostics of graphene growth induced by pulsed chemical vapor deposition. Nanoscale *5*, 6507–6517. https://doi.org/10.1039/c3nr01436c.

Shen, C., Jia, Y., Yan, X., Zhang, W., Li, Y., Qing, F., and Li, X. (2018). Effects of Cu contamination on system reliability for graphene synthesis by chemical vapor deposition method. Carbon *127*, 676–680. https://doi.org/10.1016/j.carbon.2017.11.059.

Terasawa, T.-o., and Saiki, K. (2015). Radiation-mode optical microscopy on the growth of graphene. Nat. Commun. *6*, 6834. https://doi.org/10.1038/ncomms7834.

Wang, Z.J., Weinberg, G., Zhang, Q., Lunkenbein, T., Klein-Hoffmann, A., Kurnatowska, M., Plodinec, M., Li, Q., Chi, L., Schloegl, R., and Willinger, M.G. (2015). Direct observation of graphene growth and associated copper substrate dynamics by in situ scanning electron microscopy. ACS Nano *9*, 1506–1519. https://doi.org/10.1021/nn5059826.

Wang, H., Zhao, L., Jia, Y., Li, D., Yang, L., Lu, Y., Feng, G., and Wan, W. (2020). State-of-the-art review of high-throughput statistical spatial-mapping characterization technology and its applications. Engineering *6*, 621–636. https://doi.org/10.1016/j.eng.2020.05.005.

Wilmer, C.E., Leaf, M., Lee, C.Y., Farha, O.K., Hauser, B.G., Hupp, J.T., and Snurr, R.Q. (2011). Large-scale screening of hypothetical metal–organic frameworks. Nat. Chem. *4*, 83–89. https://doi.org/10.1038/nchem.1192.

Wu, W., De, D., Chang, S.C., Wang, Y.N., Peng, H.B., Bao, J.M., and Pei, S.S. (2013). High mobility and high on/off ratio field-effect transistors based on chemical vapor deposited single-crystal $MoS_2$ grains. Appl. Phys. Lett. *102*. https://doi.org/10.1063/1.4801861.

Xiang, X.D., Sun, X.D., Briceno, G., Lou, Y.L., Wang, K.A., Chang, H.Y., Wallacefreedman, W.G., Chen, S.W., and Schultz, P.G. (1995). A combinatorial approach to materials discovery. Science *268*, 1738–1740. https://doi.org/10.1126/science.268.5218.1738.

## STAR★METHODS

### KEY RESOURCES TABLE

| REAGENT or RESOURCE | SOURCE | IDENTIFIER |
|---|---|---|
| Chemicals, peptides, and recombinant proteins | | |
| #1Copper foil (44-cm long, 50-μm thick and 7.5-cm wide, 99.9%) | CNMC Albetter Copper Co., Ltd. | CAS:7440-50-8 |
| #2Copper foil (30-cm long, 50-μm thick and 3-cm wide, 99.9%) | Lingbao Jinyuan Zhaohui Copper Co., Ltd. | CAS:7440-50-8 |
| Argon | Chengdu Qiyu Gas Co., Ltd. | 99.999% purity; CAS:7440-37-1 |
| Hydrogen/Argon | Chengdu Qiyu Gas Co., Ltd. | 5% $H_2$ diluted in Ar; CAS: 1333-74-0 |
| Methane/Argon | Chengdu Qiyu Gas Co., Ltd. | 1% $CH_4$ diluted in Ar; CAS: 7440-37-1 |
| Software and algorithms | | |
| ImageJ | | https://imagej.nih.gov/ij/ |
| Other | | |
| Optical microscopy(LV100ND) | Nikon | https://www.microscope.healthcare.nikon.com/zh_CN/products/polarizing-microscopes/eclipse-lv100nd-pol-ds |

### RESOURCE AVAILABILITY

#### Lead contact

Further information and requests for resources and reagents should be directed to and will be fulfilled by the lead contact, Xuesong Li (lxs@uestc.edu.cn)

#### Materials availability

This study did not generate new unique reagents.

#### Date and code availability

Data reported in this paper will be shared by the lead contact upon request.

No custom code was used in the analysis of the data.

### METHODS DETAILS

#### Equipment and graphene growth

*R2R CVD equipment.* A home-made R2R CVD equipment was used, which was equipped with a tube furnace and a quartz tube. The length of the furnace was 60 cm and the outer diameter of the quartz tube was 100 mm. The length of the heating element was 44 cm. 50-μm thick and 7.5-cm wide Cu strip (#1 Cu foil, from CNMC Albetter Copper Co., Ltd., 99.9% purity) was used as either a support. The #1 Cu strip was wrapped on the two rollers and moved in the same direction with the gas flow.

*Graphene synthesis.* (1) Steady reaction: A piece of 50-μm thick 3 cm × 30 cm of #2 Cu foil (Lingbao Jinyuan Zhaohui Copper Co., Ltd., 99.9% purity) was loaded on #1 Cu strip at the center of the furnace. The reaction chamber was then evacuated to <10 Pa first. Then the Cu substrate was heated up to 1030°C under 400 sccm Ar (99.999%) in 70 min, followed with a 30-min annealing process under 400 sccm $H_2$/Ar (5% $H_2$ diluted in Ar). For the steady reaction, 50 sccm $CH_4$/Ar (1% $CH_4$ diluted in Ar) was introduced while the Cu substrate began to move at a rate of 5 mm/min until it was out of heating zone. (2) Unsteady reaction: A piece of 50-μm thick and 3 cm × 30 cm of #2 Cu foil was carried out in a process similar to that of "Steady reaction". The gas parameters for graphene growth changed with time by increasing the flow rate of $CH_4$/Ar step by step from 40 to 50 and then to 60 sccm with each flow rate lasting for 50 min, 20 min, and 20 min, respectively, with Cu moving at 5 mm/min.

### Optical microscopy

Characterization was performed with optical microscopy (Nikon, LV100ND) at room temperature.

## QUANTIFICATION AND STATISTICS ANALYSIS

### Image analysis and domain number counting

The statistical results of optical images were from 3 different regions for each position. The coverage, domain size and domain density of graphene at each position was measured and counted by software *ImageJ*.